H2O2-responsive VEGF/NGF gene co-delivery nano-system achieves stable vascularization in ischemic hindlimbs

Youlu Chen
CAMS and PUMC: Chinese Academy of Medical Sciences & Peking Union Medical College
Zuoguan Chen
CAMS PUMC: Chinese Academy of Medical Sciences and Peking Union Medical College
Jianwei Duan
CAMS and PUMC: Chinese Academy of Medical Sciences & Peking Union Medical College
Liang Gui
CAMS PUMC: Chinese Academy of Medical Sciences and Peking Union Medical College
Huiyang Li
CAMS PUMC: Chinese Academy of Medical Sciences and Peking Union Medical College
Xiaoyu Liang
CAMS and PUMC: Chinese Academy of Medical Sciences & Peking Union Medical College
Xinxin Tian
CAMS and PUMC: Chinese Academy of Medical Sciences & Peking Union Medical College
Kaijing Liu
CAMS and PUMC: Chinese Academy of Medical Sciences & Peking Union Medical College
Yongjun Li
CAMS PUMC: Chinese Academy of Medical Sciences and Peking Union Medical College
Jing Yang (✉ yangjing37@hotmail.com)
CAMS PUMC: Chinese Academy of Medical Sciences and Peking Union Medical College
https://orcid.org/0000-0003-3848-5958

Research

Keywords: Vascular endothelial growth factor, Nerve growth factor, Gene therapy, Hydrogen peroxide, Angiogenesis

Posted Date: November 1st, 2021

DOI: https://doi.org/10.21203/rs.3.rs-994399/v1

Version of Record: A version of this preprint was published at Journal of Nanobiotechnology on March 19th, 2022. See the published version at https://doi.org/10.1186/s12951-022-01328-6.

H_2O_2-responsive VEGF/NGF gene co-delivery nano-system achieves stable vascularization in ischemic hindlimbs

Youlu Chen[1,†], Zuoguan Chen[2,†], Jianwei Duan[1], Liang Gui[2], Huiyang Li[1], Xiaoyu Liang[1], Xinxin Tian[1], Kaijing Liu[1], Yongjun Li[2,*], Jing Yang[1,*]

[1] Tianjin Key Laboratory of Biomaterial Research, Institute of Biomedical Engineering, Chinese Academy of Medical Science and Peking Union Medical College, 236 Baidi Road, Tianjin, 300192, P. R. China.

[2] Department of Vascular Surgery, Beijing Hospital, National Center of Gerontology, Chinese Academy of Medical Science and Peking Union Medical College, 1 Dahua Road, Beijing, 100730, P. R. China.

[*]Corresponding authors. E-mails: liyongjun4679@bjhmoh.cn; yangjing37@hotmail.com;

[†]These authors contributed equally to this work.

Abstract

Peripheral vascular disease (PVD) is a common clinical manifestation of atherosclerosis. Vascular endothelial growth factor (VEGF) gene therapy is a

promising approach for PVD treatment. However, due to single-gene therapy limitations and high H_2O_2 pathological microenvironment, VEGF gene therapy are not as expectations and its clinical application are limited. Synergistic effects of Nerve factors and vascular factors in angiogenesis have attracted attention in recent years. In this study, VEGF and nerve growth factor (NGF) genes co-delivery nanoparticles (VEGF/NGF-NPs) were prepared by using H_2O_2 responsive 6s-PLGA-Po-PEG as a carrier. 6s-PLGA-Po-PEG could react with H_2O_2 specifically due to the internal peroxalate bond. Angiogenic effects of VEGF/NGF-NPs has been evaluated in cells and hindlimb ischemia mice model. Results showed that VEGF/NGF-NPs promoted VEGF and NGF co-expression simultaneously, eliminated excessive H_2O_2, strengthened reactions between SH-SY5Ys and HUVECs, and finally enhanced migration, tube formation, proliferation and H_2O_2 damage resistance of HUVECs. VEGF/NGF-NPs also recovered blood perfusion, promoted the expression of VEGF, NGF, eNOS and NO, and enhanced vascular coverage of pericytes. Treatment effects of VEGF/NGF-NPs may related to VEGF/eNOS/NO pathway. Altogether, VEGF/NGF-NPs eliminated excessive H_2O_2 while achieving gene

co-delivery, and promoted stable angiogenesis. It's a promising way for PVD treatment by using VEGF/NGF-NPs.

Keywords: Vascular endothelial growth factor, Nerve growth factor, Gene therapy, Hydrogen peroxide, Angiogenesis

1 Introduction

Peripheral vascular disease (PVD) is one of the most common vascular diseases, which refers to non-myocardial artery obstruction or stenosis, affecting more than 200 million people worldwide. PVD often showed lower extremity blood flow damage and increased hydrogen peroxide (H_2O_2) content [1]. Blood vessel by-pass grafting and endovascular therapy have been regarded as "gold standard" among PVD treatments [2]. However, those surgeries require a long recovery time and may be associated with a variety of complications, such as graft infection, graft thrombosis, wound rupture or infection, and chronic lower extremity edema. In addition, there are many patients who don't meet the treatment conditions, and 30% of them will undergo extensive amputation [3]. These problems have brought great challenges to clinical treatment of PVD.

Gene therapy is an attractive strategy to promote angiogenesis for repairing ischemic tissue perfusion. It generates new blood vessels by transferring specific genes, such as vascular endothelial growth factor gene (pVEGF) [4-5]. VEGF is a major regulator of angiogenesis and a key factor in initiating complex cascades, which leads to the formation of new vascular networks [6]. VEGF up-regulates nitric oxide synthase (eNOS) protein level, and nitric oxide (NO) produced by eNOS significantly contributes to the prosurvival/proangiogenic program of capillary endothelium by triggering and transducing cell growth and differentiation [7-9]. However, clinical trials of pVEGF therapy have been disappointing for poor stability of neovascularization.[10] This may be due to the limitations of single-gene therapy, which is different from natural angiogenesis. Moreover, gene transfection efficiency is poor in H_2O_2 microenvironment.

Angiogenesis is a complex process involving interconnections of molecular and tissue signals, in which neural interaction is essential. It has been found that nerve growth factor (NGF), as a pleiotropic factor acting on blood vessels and nerves, promotes angiogenesis and vascular repair [10]. Therefore, co-delivery of pVEGF and NGF

gene (pNGF) in ischemic hindlimb may expect to simulate interactive support of blood vessels and nerves, and enhance stable therapeutic angiogenesis ultimately.

Oxidative stress and redox regulation are also key issues in the PVD. Reactive oxygen species (ROS) is regarded as a double-edged sword in regulating various cellular signal transduction processes. When produced ROS exceed natural level of cells, it was found to cause destruction of nucleic acids, proteins, lipids and other biological molecules, and eventually trigger cell death [11]. Among numerous kinds of ROS, hydrogen peroxide (H_2O_2) is the main component. Therefore, the use of H_2O_2 scavenging materials is expected to construct an immune microenvironment conductive angiogenesis. In our group, PLGA and PEG were covalently linked by peroxalate bonds, which could react with H_2O_2 specifically [12]. While reducing excess H_2O_2 in pathological microenvironment, NPs could realize the responsive release of genes, thus higher gene transfection efficiency could be achieved.

In this study, pVEGF and pNGF co-delivery nanoparticles (VEGF/NGF-NPs) were prepared by using 6s-PLGA-Po-PEG as carrier. The characterization of VEGF/NGF-NPs, including cellular uptake, lysosomal escape, genes transfection,

H_2O_2 scavenging, cell migration, tube formation and intercellular interactions, were evaluated *in vitro*. Therapeutic effects of VEGF/NGF-NPs in angiogenesis were also evaluated in hindlimb ischemia mice model by detecting the expression of VEGF, NGF, CD31, αSMA, NG_2, eNOS, NO, the repair of muscle tissue and the recovery of blood perfusion in ischaemic hindlimbs.

2 Materials and methods

2.1 Materials

pVEGF and pNGF were purchased from Aibimeng Biotechnology Co., Ltd (Jiangsu, China). Protamine sulfate and coumarin 6 were obtained from Aladdin (Shanghai, China). Paraformaldehyde, DAPI, MTT, RIPA Lysis Buffer, 5 × SDS-PAGE Sample Loading Buffer, 20 × TBST buffer, ECL Western Blotting Substrate and Color Mixed Protein Marker were purchased from Solarbio (Beijing, China). SDS-PAGE gel preparation kit and Lyso-Tracker were bought from Beyotime (Jiangsu, China). Hydrogen peroxide (H_2O_2, 30 wt %) was purchased from Tianjin Guangfu Fine Chemical Research Institute (Tianjin, China). 2,7-dichlorodihydrofluorescein

diacetate (DCFH-DA) was purchased from Sigma-Aldrich (St.Louis, MO, USA). Matrigel was purchased from Corning (New York, USA).

2.2 Cells and animals

The human umbilical vein endothelial cells (HUVECs) and SH-SY5Ys cell line were obtained from the Cell Bank of Chinese Academy of Sciences. HBVPs were purchased from Shanghai Yubo Biotechnology Co., Ltd. Female 6-week-old ICR mice were purchased from SPF (Beijing) Biotechnology Co., Ltd. (China) (Approval No.: SCXK(Jing): 2019-0010).

2.3 Preparation of NPs

Preparation of VEGF-NPs (or NGF-NPs): distilled water solution containing 1.5 mg protamine sulfate was slowly added into dichloromethane solution containing 80 mg 6s-PLGA-Po-PEG under ice bath condition at 20000 rpm of homogenizer. Under same conditions, distilled water solution containing 1.5 mg of pVEGF (or pNGF) was added slowly into the above solution. Under the condition of No.3 Power of homogenizer, above solution was dropwise added into 15 mL 1% PVA solution slowly and stirred for 20 min. Then, dichloromethane was removed by stirring and

volatilizing for 3 h at room temperature (RT). In this case, VEGF-NPs (NGF-NPs) were obtained.

The preparation of Blank-NPs, Coumarin-NPs and VEGF/NGF-NPs: Blank-NPs were prepared without any plasmids added; Coumarin-NPs were prepared with 8 mg coumarin 6 added to replace plasmids; VEGF/NGF-NPs were prepared by adding 1.5 mg pVEGF, 1.5 mg pNGF and 3 mg protamine sulfate. The remaining steps were the same as above.

2.4 Characterization of NPs

Size, PDI and zeta potential of NPs were measured by zeta sizer nano ZS (Malvern instruments, UK) (n=3). Stability of NPs within 25 d was determined by zeta sizer nano ZS every 5 d (n=3).

Morphology of NPs: 100 μL Blank-NPs, VEGF-NPs, NGF-NPs and VEGF/NGF-NPs suspension were dropped on copper mesh. After drying overnight, the morphology of NPs were observed by transmission electron microscopy (TEM) (h-6009iv, Hitachi).

Gene's encapsulation: Supernatant was obtained by centrifuging NPs suspension, and then agarose gel electrophoresis was used to detect whether there were unencapsulated genes in the supernatant.

Gene's release: After 2.8 mg NPs were dissolved into 4 mL PBS (or 40 μM H_2O_2 solution), placed them in 37 ℃ constant temperature shaker. On the 1, 3, 5, 8, 12, 16, 20 and 25 d, the above solutions were centrifuged at 15000 rpm to get supernatants. After supernatants were collected the same volume of PBS was added. The content of plasmid was detected by nucleic acid densitometer at 260 nm, and the cumulative release curve was drawn (n=3).

$$\text{Cumulative release (\%)} = \frac{\text{Cumulative release of pDNA}}{\text{Total mass of loaded pDNA}} \times 100\%$$

2.5 Celluar uptake and lysosomal escape of NPs

HUVECs (or SH-SY5Ys) were seeded into confocal dish at a density of 5×10^4 cells/dish. HUVECs (or SH-SY5Ys) were incubated with 62.5 μg/mL coumarin (naked-Coumarin group) or 687.5 μg/mL Coumarin-NPs (Coumarin-NPs group) for 0, 2, 4 and 6 h respectively. After cleaning with PBS for 3 times, add 400 μL Lyso-Tracker Red to each dish, incubate for 4 h, and then clean with PBS for 3 times.

After that, 500 μL 4% paraformaldehyde was added to each dish for 20 min at RT and then PBS was used to gently cleaned for 3 times. Added 300 μL DAPI dye to each dish and reacted at RT for 6 min, and then cleaned the dishes gently with PBS for 3 times. Finally, 500 μL PBS was added to each dish. Celluar uptake and lysosomal escape of Coumarin-NPs in HUVECs (or SH-SY5Ys) were observed by confocal laser scanning microscopy (CLSM 410, Zeiss, Jena, Germany).

2.6 Cytocompatibility and H_2O_2 scavenging ability

Intracellular clearance of H_2O_2: HUVECs (or SH-SY5Ys) were seeded into a confocal dish with a density of 5×10^4 cells/dish. After 24 h, HUVECs (or SH-SY5Ys) were incubated with 648.4 μg/mL Blank-NPs for 24 h. Control group was added with the same volume of serum-free medium. After that, the medium containing 10 μg/mL LPS was replaced and incubated for 2 h. The remaining H_2O_2 was determined with the amplex red assay. Finally, 500 μL PBS was added to observe the scavenging effect of Blank-NPs on intracellular H_2O_2 by confocal laser scanning microscopy (CLSM 410, Zeiss, Jena, Germany).

Response of NPs to H_2O_2 *in vitro*：After mixing 52.6 mg Blank-NPs with 10 μM H_2O_2 medium (or PBS) for 5 min, the mixed liquid was dripped onto copper mesh. Dried overnight at RT, the morphological changes were observed under TEM (h-6009iv, Hitachi). The particle size, zeta potential of NPs were measured by zeta sizer nano ZS (Malvern instruments, UK).

Cytocompatibility of Blank- NPS on HUVECs and SH-SY5Ys： HUVECs (or SH-SY5Ys) were seeded into 96-well plates at a density of 5×10^3 cells/well. After 24 h of culture, HUVECs (or SH-SY5Ys) were incubated with 0.04, 0.17, 0.68, 2.70, 10.81, 43.23, 172.92 μg/mL Blank-NPs for 24 h. Control group didn't add Blank-NPs. Then, 5 mg/mL MTT was added to each well. After 4 h, supernatant was discarded and 150 μL DMSO was added to each well. The cell plates vibrated for 5 min and the OD value of each well was detected at the wavelength of 490 nm by a Varioskan Flash microplate reader (Thermo Fisher Scientific, USA).

Cell viability $\%=\frac{\text{OD value of Blank}-\text{NPs group}}{\text{OD value of Control group}}\times100\%$

Protective effect of Blank-NPs on HUVECs in H_2O_2 solution：HUVECs were seeded into 96-well plates at a density of 5×10^3 cells/well. After 24 h of culture, HUVECs

were incubated with 10 μM H_2O_2 medium containing 0, 0.68, 0.17, 0.04, 0.01 μg/ml Blank-NPs for 24 h. Control group was added with the same volume of serum-free medium. Then, 5 mg/mL MTT 20 μL was added to each well. After 4 h, supernatant was discarded and 150 μL DMSO was added to each well. The cell plates vibrated for 5 min and the OD value of each well was detected at the wavelength of 490 nm by a Varioskan Flash microplate reader (Thermo Fisher Scientific, USA).

$$\text{Cell viability \%} = \frac{\text{OD value of H2O2 group}}{\text{OD value of Control group}} \times 100\%$$

2.7 Gene transfection of NPs

HUVECs were seeded into confocal dishes at a density of 5×10^4 cells/well for 24 h. HUVECs were then incubated with 2.68 mg/mL NPs and 96.8 μg/mL naked pVEGF or/and pNGF respectively for 48 h, and Control group was incubated with the same volume of serum-free medium. After 3 times of PBS cleaning, 500 μL 4% paraformaldehyde was added to each dish at RT for 20 min. After cleaning with PBS for 3 times, 300 μL DAPI was added to each dish. After reacting at RT for 6 min, PBS was used to clean for 3 times. Finally, 500 μL PBS was added to observe the

gene transfection results by confocal laser scanning microscopy (CLSM 410, Zeiss, Jena, Germany).

2.8 Cell migration and tube formation

Cell migration: HUVECs (or HBVPs) were seeded into 6-well plates at a density of 3 × 10^5 cells/well, and cultured for 24 h to achieve 100% fusion. Use pipette tip to make scratch wound. Wash with PBS to remove the cells under scratch. HUVECs (or HBVPs) were incubated with 0.67 mg/mL NPs and 24.2 μg/mL naked pVEGF or/and pNGF respectively for 48 h, and Control group was incubated with the same volume of serum-free medium. Cell migration was observed and photographed under inverted microscope at 12 h and 24 h respectively (n=4) and analysed by ImageJ software (National Institutes of Health, Bethesda, MD).

$$\text{Cell migration (\%)} = \frac{\text{Initial scratch area} - \text{Scratch area after cell migration}}{\text{Initial scratch area}} \times 100\%$$

Tube fomation: On the ice box, Matrigel was diluted with serum-free medium, and about 150 μL of Matrigel was added into each 24-well plate. The plate then placed into 37 ℃ incubator for 30 min to solidify the matrix. HUVECs was digested with 0.25% trypsin, and then added into serum-free medium containing 0.67 mg/mL NPs

204 or 24.2 μg/mL naked pVEGF or/and pNGF to prepare single cell suspension of 5 ×
205 10^4 cells/mL. Control group cells were added with equal volume of serum-free
206 medium. Then, HUVECs suspension was added into plate with matrix. After cultured
207 in 37 ℃ incubator for 6 h, tubule formation was observed under inverted microscope
208 and photographed (n=4) and analysed by ImageJ software (National Institutes of
209 Health, Bethesda, MD).

210 **2.9 Enhanced interaction between cells**

211 SH-SY5Ys (or HUVECs) were seeded into 6-well plates at a density of 3 × 10^5
212 cells/well, and cultured for 24 h. SH-SY5Ys (or HUVECs) were then incubated with
213 2.68 mg/mL VEGF/NGF-NPs or Serum-free medium for 24 h. After the incubation,
214 supernatant was taken and centrifuged at 4000 rpm for 10 min to get the SH-SY5Ys
215 (or HUVECs) culture supernatant (Sup) and the SH-SY5Ys (or HUVECs) culture
216 supernatant after VEGF/NGF-NPs incubation (Sup + NPs). On one hand, HUVECs
217 (or HBVPs) were incubated in serum-free medium or 10 μM H_2O_2 medium with Sup
218 or Sup + NPs for 24 h, and Control group was incubated with the same volume of
219 serum-free medium to test cell proliferation ability followed the method in 2.6. On the

other hand, HUVECs (or HBVPs) were incubated with Sup or Sup + NPs for 12 h and 24 h, and Control group was incubated with the same volume of serum-free medium to test cell migration ability Followed the method in 2.8.

2.10 Blood perfusion and histological detection of hindlimbs

Female ICR mice (6-week-old) were divided into 8 groups randomly: Control group (PBS), VEGF group (naked VEGF), NGF group, VEGF + NGF group (naked NGF), Blank-NPs group, VEGF-NPs group, NGF-NPs group and VEGF/NGF-NPs group. Mice were anesthetized by intraperitoneal injection of chloral hydrate (400 mg/kg) and the femoral artery of mice was excised from inguinal ligament to bifurcation of saphenous artery and popliteal artery under general anesthesia. On the 1st, 3rd, 5th, 7th, 9th, 11th and 13th day, 0.67 mg/mL NPs and 24.2 μg/mL pVEGF or/and pNGF were injected intramuscularly. PBS injection was used as control. On the 1st, 4th, 7th, 14th, 21st and 28th day after surgery, the blood perfusion of the hind limbs was monitored by Laser Doppler Flowmeter (PERIMED AB, Sweden) and results were analyzed by PIMSOFT software (PERIMED AB, Sweden) (n=5). After sacrifice of mice, ischemic muscle was detected by Haematoxylin and Eosin (H&E) staining and

Masson staining. Angiogenesis was detected by CD31 immunohistochemistry and vascular stability was detected by CD31, NG2, α-SMA, DAPI immunofluorescence staining.

2.11 VEGF, NGF, eNOS and NO expression assay

After homogenized in 400 μL of lysis buffer, the lysates of ischaemic tissues were centrifuged at 10000 rpm for 15 min. Equal amounts of total proteins (15 μg) collected from supernatants were electrophoresed on 10% polyacrylamide gels. Then, proteins were transferred to PVDF membranes. After that, PVDF membranes were incubated with VEGF, NGF and eNOS antibodies followed by a HRP-conjugated anti-goat secondary antibody. Super Signal Ultra chemiluminescent reagent (Pierce, Rockford, IL) was used to detecte protein immunoblot signals. The expression level of the VEGF, NGF and eNOS protein was quantified with ImageJ software (n=5). NO was detected by NO ELISA Kit (Shanghai Lanpai Biotechnology Co., Ltd, China).

2.11 Statistical analysis

Statistical significance between multiple groups were performed with one-way ANOVA. Data are expressed as the mean ± standard deviation. Differences with a value of $P < 0.05$ were considered statistically significant.

3 Results

3.1 Preparation and characterization of NPs

Gene NPs were prepared by high speed stirring double emulsion method (Figure 1A), GFP plasmid (pGFP) was used as a report gene. To increase the gene loading rate in NPs, positively charged protamine was added, which could combine plasmids and NPs by electrostatic interaction. As is shown in Figure 1C, we prepared protamine loaded GFP-NPs (with pro group) and protamine free GFP-NPs (without pro group) respectively. Meanwhile, GFP-NPs (with pro) were dissolved in dichloromethane and were extracted to release the inside plasmids with distilled water (NP's extract group). Agarose gel electrophoresis was used to detect NP's extracted solution and supernatant after centrifugation of NPs. It could be seen that pGFP was fully packed into NPs by adding protamine. In addition, the pGFP remained integral in the process of preparation without fragmentation.

In accordance with the foregoing method, Blank-NPs (without plasmids), VEGF-NPs (containing 1.5 mg pVEGF), NGF-NPs (containing 1.5 mg pNGF) and VEGF/NGF-NPs (containing 1.5 mg pVEGF and 1.5 mg pNGF) were prepared respectively. Morphology of NPs were observed by TEM. It could be seen that NPs were spherical with a layer of small spherical particles adsorbed on the surface. This phenomenon may be caused by the formation of complex between protamine and plasmid and adsorption on NPs surface. (Figure 1B). By detecting the supernatant, there were no leaked genes (Figure 1D). Therefore, both pVEGF and pNGF were encapsulated completely. Particle size, PDI and zeta potential of NPs were also detected. Particle sizes of Blank-NPs, VEGF-NPs, NGF-NPs and VEGF/NGF-NPs were (258.4 ± 7.6) nm, (244.9 ± 13.6) nm, (231.8 ± 6.5) nm and (205.2 ± 1.9) nm, respectively. PDI were 0.226 ± 0.036, 0.273 ± 0.008, 0.273 ± 0.008 and 0.217 ± 0.008, and zeta potential were - (2.70 ± 0.16) mV, - (5.03 ± 0.95) mV, - (6.70 ± 0.49) mV and - (11.27 ± 1.65) mV respectively (Figure 1E). In addition, NPs were stable within 25 days (Figure 1F).

3.2 H_2O_2 scavenging and pVEGF/pNGF co-transfection of NPs

Polymer-based gene delivery systems have been reported widely [13-15]. Gene delivery systems usually need to be more easily uptaken by cells, achieving lysosomal escape, releasing genes and scavenging H_2O_2 successfully in cells [16-18]. Therefore, H_2O_2 scavenge ability and gene delivery process of VEGF/NGF-NPs were explored.

Firstly, morphology, particle size and zeta potential of NPs in H_2O_2 environment were observed to explore H_2O_2 responsiveness of NPs. Results showed that NPs was obviously broken in 10 μm H_2O_2 solution. Schematic diagram and representative images of TEM were shown (Figure 2A&B). Particle size results showed that small particle fragments increased with time, proving that fragmentation of NPs was occurring continuously (Figure 2C). Zeta potential results showed that surface charge of Blank-NPs changed from a large peak to three small peaks, including the same peak as the original peak, the peak with large negative charge and the peak with positive charge (Figure 2D). These two new peaks may be caused by the release of protamine after NPs reacted with H_2O_2. In addition, gene's release was accelerated in H_2O_2 environment comparing to PBS environment, indicating that gene release was

297 intensified after NPs' broken (Figure 2E&F). These results indicated that NPs was

298 H_2O_2 responsive and could be broken after reacting with H_2O_2.

299 Then, to explore gene delivery process of VEGF/NGF-NPs (Figure 3A),

300 cytocompatibility, cellular uptake, lysosomal escape, intracellular H_2O_2 clearance, cell

301 protection and gene transfection of NPs were explored. Cytocompatibility of NPs was

302 tested in HUVECs and SH-SY5Ys, and results showed that NPs had almost no

303 toxicity to both type of cells (Figure 2G&H). Coumarin-NPs were prepared by

304 loading coumarin 6 to observe the uptake of NPs by HUVECs. Compared with

305 naked-Coumarin group, Coumarin-NPs could be absorbed more by HUVECs within

306 the same amount of time (Figure 3B), and Coumarin 6-NPs also achieved lysosomal

307 escape successfully (Figure 3C). H_2O_2 scavenging and cell protection of NPs were

308 also detected in HUVECs. In Figure 3D, compared with Control group, Blank-NPs

309 attenuated ROS increasing successfully in HUVECs induced by LPS. After that,

310 protection of NPs on HUVECs in H_2O_2 medium was also tested. Compared with H_2O_2

311 group, Blank-NPs resisted H_2O_2 injury on HUVECs effectively, and the protection

312 was enhanced when NP’s concentration increased (Figure 2H). Finally, gene

transfection efficiency of NPs was investigated. To facilitate observation, VEGF-RFP plasmids and NGF-GFP plasmids with fluorescent protein were constructed by using PAAV-G-CMV-2A-RFP-blank and PAAV-G-CMV-2A-GFP-blank vectors. After co-delivery, transfecation efficiency of NPs was observed in confocal laser scanning microscopy. Compared with free pVEGF and pNGF, delivery through NPs achieved more efficient pVEGF and pNGF transfection. More importantly, VEGF/NGF-NPs realized simultaneous and efficient co-transfection of pVEGF and pNGF (Figure 3F).

3.3 VEGF/NGF-NPs promoted cell migration and tubulogenesis of HUVECs

Enhancement of endothelial cell migration and tubulogenesis is crucial to angiogenesis [19]. Therefore, we detected tubule formation and migration of HUVECs incubated by NPs, and representative images were given (Figure 4A&D). Compared with Control group, VEGF group and VEGF+NGF group didn't seem to promote tube formation or migration of HUVECs, while VEGF-NPs group and VEGF/NGF-NPs group promoted relative tube length, relative meshed area and HUVECs migration obviously. Compared with VEGF+NGF group, VEGF/NG-NPs promoted tube formation and cell migration significantly, which indicated that this

gene delivery system enhanced function of its inside genes through efficient transfection. In addition, compared with VEGF-NPs group, VEGF/NGF-NPs group didn't promote the relative tube length, but promoted the relative meshed area visibly, implying that co-delivery of pNGF assisted pVEGF in accelerating vascular network formation of HUVECs (Figure 4B&C). And compared with VEGF-NPs group, differences of HUVECs migration in VEGF/NGF-NPs group were little in 24 h. Co-delivery of pNGF to help pVEGF on HUVECs migration was limited (Figure 4E&F).

3.4 VEGF/NGF-NPs promoted intercellular interactions

Nutrition of nerve plays an important role in the process of ischemic tissue repair. If interactions between nerve and blood vessel enhanced, it's hopeful to get further angiogenesis and ischemic repair [20-21]. Therefore, we investigated whether VEGF/NGF-NPs had the potential to promote interactions between nerve and blood vessel. In this study, SH-SY5Ys were incubated with VEGF/NGF-NPs and supernatant after centrifuging (Sup+NPs) were collected *in vitro*, and then HUVECs were incubated with Sup+NPs to simulate the interaction process (Figure 5A).

Before that experiment, we first detected cellular uptake (Figure 5B), lysosomal escape (Figure 5C) and H_2O_2 clearance (Figure 5D) of NPs in SH-SY5Ys. It could be seen that NPs achieved lysosomal escape and higher cellular uptake in SH-SY5Ys. Meanwhile, NPs also removed excessive ROS in SH-SY5Ys caused by LPS (Figure 5D). Therefore, the gene delivery system was also feasible for SH-SY5Ys. Then, we examined the effects of Sup+NPs on migration, proliferation and H_2O_2 resistance of HUVECs. Firstly, we presented representative images of HUVECs migration results (Figure 5E). Compared with Control group, Sup+NPs group promoted cell migration significantly at 12 h and 24 h, and the effects increased with time (Figure 5F&G). Next results showed that HUVECs proliferation in Sup+NPs group was 2.05 times as much as that in Control group (Figure 5H). Even under the influence of H_2O_2, HUVECs proliferation in Sup+NPs group was 1.66 times as much as that in Control group (Figure 5I). Sup+NPs could still promote HUVECs proliferation under H_2O_2 injury. These results indicated that VEGF/ NGF-NPs enhanced interactions between SH-SY5Ys and HUVECs and further promoted migration, proliferation, H_2O_2 resistance of HUVECs markedly.

Pericyte coverage is crucial to the stability of neovascularization, therefore, interactions between HUVECs and HBVPs after VEGF/NGF-NPs transfection have been also explored. HUVECs were incubated with VEGF/NGF-NPs, and centrifuged supernatant (Sup+NPs) was collected *in vitro*, then HBVPs were incubated with Sup+NPs to simulate interaction process (Figure 6A). Results showed that compared with Control group, cell proliferation (Figure 6B) and migration (Figure 6C&D) of HBVPs in Sup+NPs group was significantly promoted, even in H_2O_2 environment. These results suggested that VEGF/NGF-NPs also enhanced interactions between HUVECs and HBVPs, and further promoted migration, proliferation and anti-H_2O_2 damage ability of HBVPs.

3.5 VEGF/NGF-NPs promoted stable angiogenesis in ischemic hindlimbs

Effects of VEGF/NGF-NPs on angiogenesis *in vivo* was detected. By establishing ICR mouse model of ischaemic hindlimb, we used five-point intramuscular injection of VEGF/NGF-NPs to promote angiogenesis (Figure 7A). Figure 7B showed representative blood flow images after 28 d of ischemia. Compared to 21 d, blood flow decreased on 28 d in all groups except VEGF/NGF-NPs group, which may be

due to the poor stability of neovascularization (Figure 7C). Compared with Control group and VEGF-NPs group, blood flow of VEGF/NGF-NPs group recovered significantly on 28 d (Figure 5D). Then H&E staining and Masson staining were performed on ischemic tissue. It could be seen that size and shape of muscle fibers in VEGF-NPs group and VEGF/NGF-NPs group were both uniform. Both VEGF-NPs and VEGF/NGF-NPs improved muscle injury and reduced the production of collagen fiber obviously (Figure 8A&B).

To observe the neovascularization more intuitively, we detected CD31 expression in ischemic tissues by immunohistochemistry, and representative pictures were given (Figure 9A). Compared with Control group and VEGF-NPs group, VEGF/NGF-NPs group promoted the expression of CD31 significantly, indicating that VEGF/NGF-NPs promoted angiogenesis in ischemic tissue significantly. During this process, pNGF and pVEGF played a synergistic role. The coverage of smooth muscle cells and pericytes often reflects the maturation and stability of neovascularization. To explore neovascularization stability, we stained ischemic tissues by immunofluorescence to co-located CD31, α-SMA (marker of smooth muscle cells),

DAPI and NG2 (marker of pericytes) of the vessels, and gave the representative picture (Figure 9B). The results showed that functional vessels (10 μm - 70 μm) in Control group and Blank-NPs group were less. Pericytes coverage of VEGF group, NGF group, VEGF+NGF group, VEGF-NPs group and NGF-NPs group were insufficient (white arrow) while VEGF/NGF-NPs group had relatively complete pericytes coverage. These results suggested that pNGF and pVEGF promoted stable angiogenesis in a synergistic manner.

3.6 VEGF/NGF-NPs enhanced the expression of VEGF, NGF, eNOS and NO

Nitric oxide (NO) produced by endothelial cells through endothelial nitric oxide synthase (eNOS) is an important vasoactive compound [22-24]. NO is responsible for a variety of physiological and cellular processes, including endothelial cell migration, proliferation and angiogenesis. The function and activity of eNOS in endothelial cells are crucial to vascular integrity and homeostasis [25-26]. In addition, studies have shown that NGF could improve angiogenesis through VEGF/Akt/NO dependent mechanism [27]. Therefore, expressions of VEGF (Figure 10A), NGF (Figure 10B), eNOS (Figure 10C) and NO (Figure 10D) in ischemic tissues were detected after

VEGF/NGF-NPs treatment. It could be seen that VEGF/NGF-NPs enhanced the expression of VEGF, NGF, eNOS and NO in ischaemic hindlimb compared with Control group (4.16, 4.15, 6.17 and 4.13 times of Control group, respectively). It should be noted that compared with VEGF-NPs group (or NGF-NPs group), VEGF/NGF-NPs didn't promote further expression of VEGF (or NGF) in ischemic lower limbs, but the expression of eNOS and NO was significantly promoted. This result may suggest that synergistic effect of pNGF helped pVEGF promoting more expressions of eNOS and NO.

4 Discussion

Angiogenesis is an important adaptive mechanism against ischemia [28-30]. Angiogenesis through gene therapy is undoubtedly a promising method for the treatment of PVD. pVEGF therapy has brought a brief promise to people, but has failed to achieve satisfactory clinical results. Strong overexpression of VEGF by different gene therapy vectors induces the growth of abnormal hemangiomatous vascular structures in skeletal muscle. Low expression of VEGF is safe, but not sufficient to produce an effective therapeutic benefit. Appropriate VEGF angiogenic

425 stimulation is needed, but the new vessels need to survive for a long time after the end
426 of angiogenic stimulation to have a real therapeutic effect on PVD. Therefore, it's
427 particularly important to promote stable angiogenesis.
428 After the budding of angiogenesis, original vascular plexus is remodeled extensively.
429 The remaining vessels are matured and stable, which marks the end of vascular
430 plasticity [31-32]. Vascular stability requires vascular maturation through recruitment
431 of parietal cells (like pericytes and smooth muscle cells) and establishment of
432 intercellular contact between parietal cells and the endothelium. In addition, pericytes
433 have long been considering to be the main regulator of vascular maturation and
434 stability, and the association with pericytes is necessary to make vessels independent
435 of sustained VEGF expression [33-35]. Among many tissues and signaling molecules
436 that influence the maturation and stability of new blood vessels, neural fiber network
437 is an important part that cannot be ignored. Vascular circulatory system and neural
438 fiber network have similar shape distribution and close ties, so strengthening the
439 interactions between them is conducive to stable angiogenesis. NGF was first isolated
440 from nervous tissue, it's one kind of pleiotropic factor that can act on both nerves and

441 blood vessels. Studies have shown that NGF stimulation increased the expression of
442 Notch1 in a dose-dependent manner, which activated the Notch signaling pathway.
443 And Notch signaling pathway plays a key role in pericytes survival [36-39]. However,
444 it's unknown whether NGF promotes stable angiogenesis through its influence on
445 pericytes, and our study has answered this question. pNGF as the co-delivery gene of
446 pVEGF enhanced the recruitment of pericytes and strengthened the stability of
447 neovascularization in 28 d. Notably, compared with pVEGF, co-delivery of pNGF in
448 ischemic hindlimbs promoted pericyte recruitment. In future studies, using gene
449 therapy to promote the recruitment and coverage of pericytes may be an effective way
450 to promote stable angiogenesis.
451 For stable angiogenesis, protective gene delivery vector for genes is equally important.
452 In this study, we synthesized 6s-PLGA-Po-PEG which eliminated H_2O_2. NPs based
453 on 6s-PLGA-Po-PEG protected genes from oxidative damage and improved the
454 microenvironment of cells by decreasing H_2O_2. In this study, the removal of H_2O_2
455 from the microenvironment by NPs was not complete, and it was still difficult to

456 restore the lower limb steady-state microenvironment. In future, carrier with the
457 ability to regulate H_2O_2 in microenvironment should be explored.
458 Co-therapy of pVEGF with a second gene has been studied by many researchers to
459 promote stable angiogenesis. Through the co-delivery of pNGF and pVEGF, Bin Gao
460 et al. found that gene expressions of double genome group were significantly
461 increased at mRNA and protein levels, which was at least 2 and 1.5 times of that in
462 single genome group respectively. Moreover, they confirmed that co-delivery of two
463 genes had a synergistic effect, which enhanced the proliferation, migration and
464 angiogenesis of HUVECs significantly [40]. Aiki Marushima et al. achieved better
465 hemodynamic recovery and ischemic protection through the co-delivery of VEGF and
466 PDGF-BB, and increased collateral blood flow of chronic hypoperfusion [41]. Our
467 study proved that, co-delivery of pVEGF and pNGF had better therapeutic efficiency
468 on the stable angiogenesis of ischemic hindlimb. In numerous studies, co-therapy of
469 pVEGF and a second gene had achieved "1+1>2" therapeutic effect. In the future,
470 combination of polygene therapy and microenvironment improvement may enable

gene NPs more functions, which is expected to become a promising way in PVD treatment.

5 Conclusion

In summary, we used H_2O_2 responsive 6s-PLGA-Po-PEG to co-loading pVEGF and pNGF and prepared VEGF/NGF-NPs. VEGF/NGF-NPs eliminated H_2O_2 while co-delivering pVEGF and pNGF, promoted stable neovascularization in ischemic hindlimbs successfully by strengthening cell interactions between nerves and blood vessels. Therefore, co-gene delivering NPs that simultaneously enhance neurovascular interactions and improve H_2O_2 microenvironment may be a promising strategy to achieve stable angiogenesis in PVD treatment.

Acknowledgments

You-Lu Chen and Zuo-Guan Chen contributed equally to this work. We acknowledge financial support from the National Natural Science Foundation of China (82072080, 31771097, 81870351), CAMS Innovation Fund for Medical Sciences (2017-12M-1-016, 2018-12M-1-002), Tianjin Research Program of Application Foundation and Advanced Technology (17JCZDJC37400), National Key Research

and Development Project (2018YFC2000300), and PUMC Discipline Construction Project (201920102101). This project was also supported by the Special Program for High-Tech Leader & Teams of Tianjin Government and the Tianjin innovation Promotion Plan Key Innovation Team of Immunoreactive Biomaterials.

Author contributions

Youlu Chen: Methodology, Validation, Formal analysis, Roles, Writing - original draft. **Zuoguan Chen:** Methodology, Validation, Formal analysis, Roles, Writing - original draft. **Jianwei Duan:** Investigation, Resources. **Liang Gui:** Investigation, Resources. **Huiyang Li:** Formal analysis, Data curation. **Xiaoyu Liang:** Investigation, Resources. **Xinxin Tian:** Investigation, Resources. **Kaijing Liu:** Formal analysis, Data curation. **Yongjun Li:** Writing - review & editing. **Jing Yang:** Conceptualization, Writing - review & editing, Project administration, Funding acquisition.

Availability of data and materials

The data that support the findings of this study are available from the corresponding author upon reasonable request.

Declarations

Ethics approval and consent to participate

All animal experiments were carried out in accordance with the relevant guidelines and regulations approved by the Center of Tianjin Animal Experiment ethics committee and authority for animal protection. (License for use of experimental animals: Approval No.: SYXK (Jin):2019-0002)

Consent for publication

All the authors agree with the publication.

Competing interest

The authors declare that they have no known competing financial interests or personal relationships that could have appeared to influence the work reported in this paper.

References

1. E. Shabani Varaki, G.D. Gargiulo, S. Penkala, P.P. Breen, Peripheral vascular disease assessment in the lower limb: a review of current and emerging non-invasive diagnostic methods, *Biomed. Eng. Online.* 17(1) (2018) 61.

518 2. Y. Xie, Y. Guan, S.H. Kim, M.W. King, The mechanical performance of
519 weft-knitted/electrospun bilayer small diameter vascular prostheses, *J. Mec.h Behav.*
520 *Biomed. Mater.* 61 (2016) 410-418.
521 3. G.V. Shrikhande, J.F. McKinsey, Use and abuse of atherectomy: where should it be
522 used? *Semin. Vasc. Surg.* 21(4) (2008) 204-9.
523 4. M. Giacca, S. Zacchigna, VEGF gene therapy: therapeutic angiogenesis in the
524 clinic and beyond, *Gene. Ther.* 19(6) (2012) 622-9.
525 5. J. Kastrup, Gene therapy and angiogenesis in patients with coronary artery disease,
526 Expert. Rev. *Cardiovasc. Ther.* 8(8) (2010) 1127-38.
527 6. A. Uccelli, T. Wolff, P. Valente, N. Di Maggio, M. Pellegrino, L. Gurke, A. Banfi,
528 R. Gianni-Barrera, Vascular endothelial growth factor biology for regenerative
529 angiogenesis, *Swiss. Med. Wkly.* 149 (2019) w20011.
530 7. B.Q. Shen, D.Y. Lee, T.F. Zioncheck, Vascular endothelial growth factor governs
531 endothelial nitric-oxide synthase expression via a KDR/Flk-1 receptor and a protein
532 kinase C signaling pathway, *J. Biol. Chem.* 274(46) (1999) 33057-63.

533 8. A. Bouloumie, V.B. Schini-Kerth, R. Busse, Vascular endothelial growth factor
534 up-regulates nitric oxide synthase expression in endothelial cells, *Cardiovasc. Res.*
535 41(3) (1999) 773-80.
536 9. Y. Zhao, P.M. Vanhoutte, S.W. Leung, Vascular nitric oxide: Beyond eNOS, *J.*
537 *Pharmacol. Sci.* 129(2) (2015) 83-94.
538 10. F. Sanada, Y. Taniyama, Y. Kanbara, R. Otsu, Y. Ikeda-Iwabu, M. Carracedo, H.
539 Rakugi, R. Morishita, Gene therapy in peripheral artery disease, *Expert. Opin. Biol.*
540 *Ther.* 15(3) (2015) 381-90.
541 11. B. Nico, D. Mangieri, V. Benagiano, E. Crivellato, D. Ribatti, Nerve growth
542 factor as an angiogenic factor, *Microvasc. Res.* 75(2) (2008) 135-41.
543 12. L. Ni, T. Li, B. Liu, X. Song, G. Yang, L. Wang, S. Miao, C. Liu, The protective
544 effect of Bcl-xl overexpression against oxidative stress-induced vascular endothelial
545 cell injury and the role of the Akt/eNOS pathway, *Int. J. Mol. Sci.* 14(11) (2013)
546 22149-62.

13. C. Liu, X. Zhu, X. Wang, D. Miao, X. Liang, C. Wang, L. Pang, H. Sun, D. Kong, J. Yang, Hydrogen peroxide-responsive micelles self-assembled from a peroxalate ester-containing triblock copolymer, *Biomater. Sci.* 4(2) (2016) 255-7.

14. C.K. Chen, P.K. Huang, W.C. Law, C.H. Chu, N.T. Chen, L.W. Lo, Biodegradable Polymers for Gene-Delivery Applications, *Int. J. Nanomedicine.* 15 (2020) 2131-2150.

15. M. Ramezani, M. Ebrahimian, M. Hashemi, Current Strategies in the Modification of PLGA-based Gene Delivery System, *Curr. Med. Chem.* 24(7) (2017) 728-739.

16. Q. Cai, L. Wang, G. Deng, J. Liu, Q. Chen, Z. Chen, Systemic delivery to central nervous system by engineered PLGA nanoparticles, *Am. J. Transl. Res.* 8(2) (2016) 749-64.

17. C. Zylberberg, K. Gaskill, S. Pasley, S. Matosevic, Engineering liposomal nanoparticles for targeted gene therapy, *Gene. Ther.* 24(8) (2017) 441-452.

18. W. Jin, M. Al-Dulaymi, I. Badea, S.C. Leary, J. Rehman, A. El-Aneed, Cellular Uptake and Distribution of Gemini Surfactant Nanoparticles Used as Gene Delivery Agents, *AAPS. J.* 21(5) (2019) 98.

563 19. J. Jo, Y. Tabata, How controlled release technology can aid gene delivery, *Expert.*

564 *Opin. Drug. Deliv.* 12(10) (2015) 1689-701.

565 20. A. Robinet, A. Fahem, J.H. Cauchard, E. Huet, L. Vincent, S. Lorimier, F.

566 Antonicelli, C. Soria, M. Crepin, W. Hornebeck, G. Bellon, Elastin-derived peptides

567 enhance angiogenesis by promoting endothelial cell migration and tubulogenesis

568 through upregulation of MT1-MMP, *J. Cell. Sci.* 118(Pt 2) (2005) 343-56.

569 21 M. Guang, Y. Yao, L. Zhang, B. Huang, L. Ma, L. Xiang, J. Jin, P. Gong, The

570 effects of nerve growth factor on endothelial cells seeded on different titanium

571 surfaces, *Int. J. Oral. Maxillofac. Surg.* 44(12) (2015) 1506-13.

572 22. N. Hansen-Algenstaedt, P. Algenstaedt, C. Schaefer, A. Hamann, L. Wolfram, G.

573 Cingoz, N. Kilic, B. Schwarzloh, M. Schroeder, C. Joscheck, L. Wiesner, W. Ruther,

574 S. Ergun, Neural driven angiogenesis by overexpression of nerve growth factor,

575 *Histochem. Cell. Biol.* 125(6) (2006) 637-49.

576 23. D. Perez-Cremades, C. Bueno-Beti, J.L. Garcia-Gimenez, J.S. Ibanez-Cabellos, C.

577 Hermenegildo, F.V. Pallardo, S. Novella, Extracellular histones disarrange vasoactive

578 mediators release through a COX-NOS interaction in human endothelial cells, *J. Cell.*
579 *Mol. Med.* 21(8) (2017) 1584-1592.
580 24. C.A. Dias-Junior, S.B. Cau, J.E. Tanus-Santos, [Role of nitric oxide in the control
581 of the pulmonary circulation: physiological, pathophysiological, and therapeutic
582 implications], *J. Bras. Pneumol.* 34(6) (2008) 412-9.
583 25. J.E. Church, D. Fulton, Differences in eNOS activity because of subcellular
584 localization are dictated by phosphorylation state rather than the local calcium
585 environment, *J. Biol. Chem.* 281(3) (2006) 1477-88.
586 26. C.A. Meza, J.D. La Favor, D.H. Kim, R.C. Hickner, Endothelial Dysfunction: Is
587 There a Hyperglycemia-Induced Imbalance of NOX and NOS? *Int. J. Mol. Sci.* 20(15)
588 (2019).
589 27. U. Forstermann, W.C. Sessa, Nitric oxide synthases: regulation and function, *Eur.*
590 *Heart. J.* 33(7) (2012) 829-37, 837a-837d.
591 28. C. Emanueli, M.B. Salis, A. Pinna, G. Graiani, L. Manni, P. Madeddu, Nerve
592 growth factor promotes angiogenesis and arteriogenesis in ischemic hindlimbs,
593 *Circulation.* 106(17) (2002) 2257-62.

29. G. Lorier, C. Tourino, R.A. Kalil, Coronary angiogenesis as an endogenous response to myocardial ischemia in adults, *Arq. Bras. Cardiol.* 97(6) (2011) e140-8.

30. S. Yuan, C.G. Kevil, Nitric Oxide and Hydrogen Sulfide Regulation of Ischemic Vascular Remodeling, *Microcirculation.* 23(2) (2016) 134-45.

31. E. Toyota, T. Matsunaga, W.M. Chilian, Myocardial angiogenesis, *Mol. Cell. Biochem.* 264(1-2) (2004) 35-44.

32. P. Barbacena, J.R. Carvalho, C.A. Franco, Endothelial cell dynamics in vascular remodelling, *Clin. Hemorheol. Microcirc.* 64(4) (2016) 557-563.

33. C.C. Huang, N.D. Lawson, B.M. Weinstein, S.L. Johnson, reg6 is required for branching morphogenesis during blood vessel regeneration in zebrafish caudal fins, *Dev. Biol.* 264(1) (2003) 263-74.

34. D. von Tell, A. Armulik, C. Betsholtz, Pericytes and vascular stability, *Exp. Cell. Res.* 312(5) (2006) 623-9.

35. C. Liu, H.M. Ge, B.H. Liu, R. Dong, K. Shan, X. Chen, M.D. Yao, X.M. Li, J. Yao, R.M. Zhou, S.J. Zhang, Q. Jiang, C. Zhao, B. Yan, Targeting pericyte-endothelial cell crosstalk by circular RNA-cPWWP2A inhibition aggravates

610 diabetes-induced microvascular dysfunction, *Proc. Natl. Acad. Sci. U. S. A.* 116(15)
611 (2019) 7455-7464.
612 36. A.M. Figueiredo, P. Villacampa, R. Dieguez-Hurtado, J. Jose Lozano, P. Kobialka,
613 A.R. Cortazar, A. Martinez-Romero, A. Angulo-Urarte, C.A. Franco, M. Claret, A.M.
614 Aransay, R.H. Adams, A. Carracedo, M. Graupera, Phosphoinositide
615 3-Kinase-Regulated Pericyte Maturation Governs Vascular Remodeling, *Circulation.*
616 142(7) (2020) 688-704.
617 37. J.C. Park, I.B. Chang, J.H. Ahn, J.H. Kim, J.H. Song, S.M. Moon, Y.H. Park,
618 Nerve Growth Factor Stimulates Glioblastoma Proliferation through Notch1 Receptor
619 Signaling, *J. Korean. Neurosurg. Soc.* 61(4) (2018) 441-449.
620 38. K. Yamamizu, M. Iwasaki, H. Takakubo, T. Sakamoto, T. Ikuno, M. Miyoshi, T.
621 Kondo, Y. Nakao, M. Nakagawa, H. Inoue, J.K. Yamashita, In Vitro Modeling of
622 Blood-Brain Barrier with Human iPSC-Derived Endothelial Cells, Pericytes, Neurons,
623 and Astrocytes via Notch Signaling, *Stem. Cell. Reports.* 8(3) (2017) 634-647.
624 39. T. Nadeem, W. Bogue, B. Bigit, H. Cuervo, Deficiency of Notch signaling in
625 pericytes results in arteriovenous malformations, *JCI. Insight.* 5(21) (2020).

626 40. B. Gao, X. Wang, M. Wang, X.K. Ren, J. Guo, S. Xia, W. Zhang, Y. Feng, From
627 single to a dual-gene delivery nanosystem: coordinated expression matters for
628 boosting the neovascularization in vivo, *Biomater. Sci.* 8(8) (2020) 2318-2328.
629 41. A. Marushima, M. Nieminen, I. Kremenetskaia, R. Gianni-Barrera, J. Woitzik, G.
630 von Degenfeld, A. Banfi, P. Vajkoczy, N. Hecht, Balanced single-vector co-delivery
631 of VEGF/PDGF-BB improves functional collateralization in chronic cerebral
632 ischemia, *J. Cereb. Blood. Flow. Metab.* 40(2) (2020) 404-419.

633 **Figures**

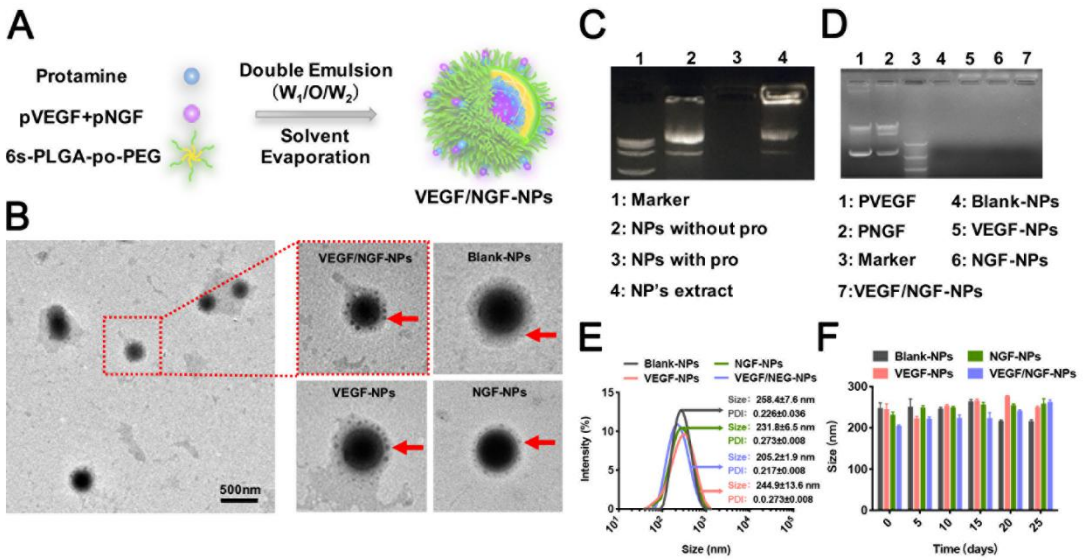

634

635 Figure 1. Characterization of NPs. (A) Schematic illustration of NP's preparation. (B)
636 Typical images of NPs under TEM. (C) Encapsulation efficiency of NPs with
637 protamine sulfate. Without pro group stands for protamine free NPs, with pro group

638 stands for protamine loaded NPs and NP's extract group stands for plasmids extract

639 after protamine loaded NPs dissolving in dichloromethane. (D) Encapsulation

640 efficiency of gene NPs. (E) Particle size of NPs. (F) Stability of NPs within 25 d. The

641 data are presented as mean ± SD (n=3).

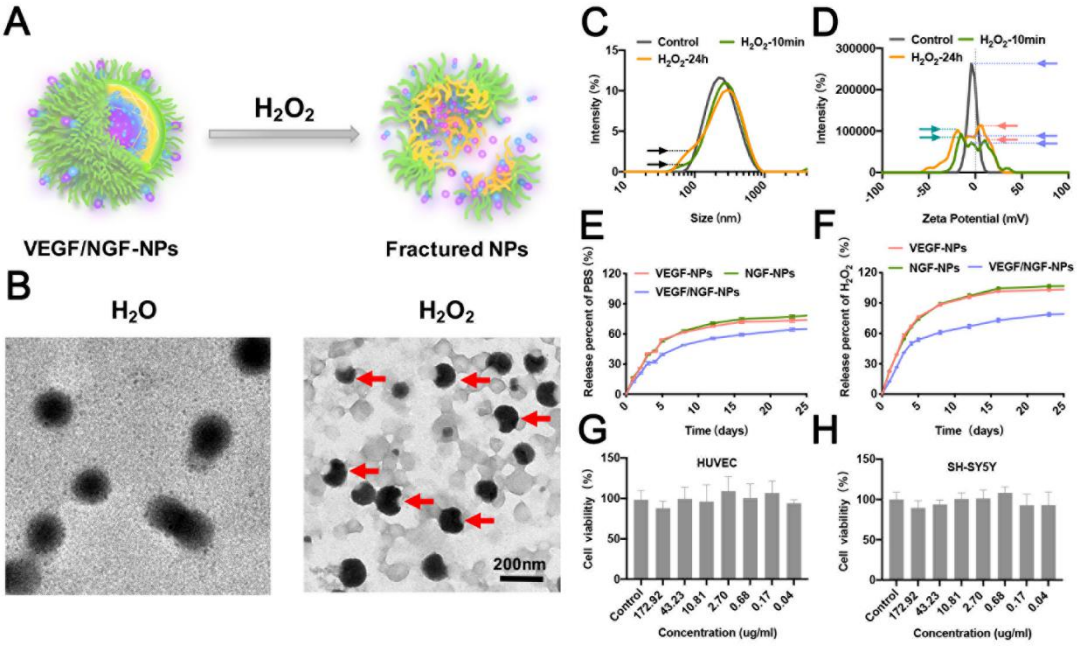

642

643 Figure 2. H_2O_2 responsiveness and biocompatibility of NPs

644 (A) Schematic illustration of NP's responsiveness to H_2O_2. (B) Typical images of NPs

645 in H_2O or H_2O_2 under TEM. Particle size (C) and surface potential change (D) of

646 Blank-NPs in PBS or H_2O_2. Genes release of NPs during 25 d in PBS (E) or H_2O_2 (F).

647 Biocompatibility of NPs when incubated with HUVECs and SH-SY5Ys.

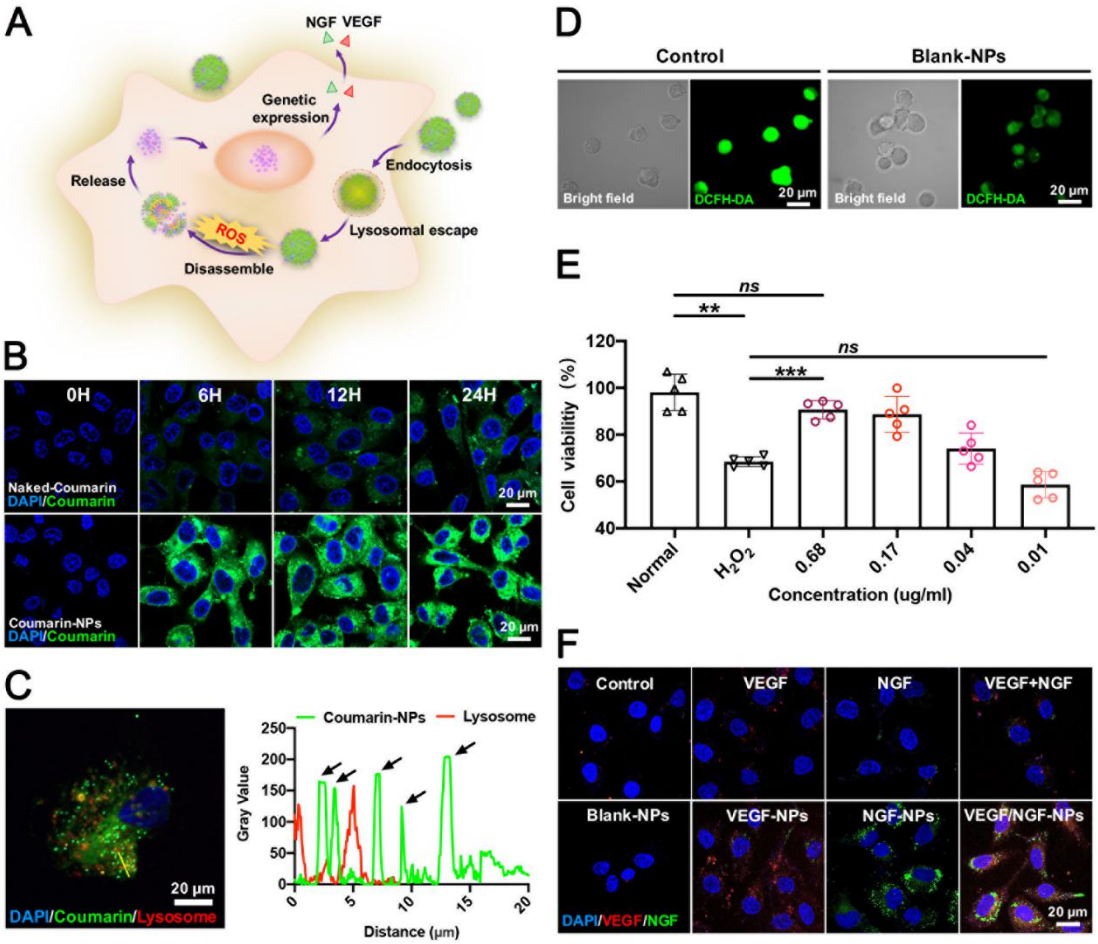

Figure 3. H_2O_2 scavenging and gene transfection of NPs in HUVECs. (A) Schematic illustration of NP's ROS scavenging and pVEGF/pNGF co-transfection in cells. (B) Cellular uptake of naked-Coumarin and Coumarin-NPs for 0 h, 6 h, 12 h and 24 h. (C) Lysosomal escape of Coumarin-NPs. (D) H_2O_2 scavenging of HUVECs after incubating Blank-NPs 24 h in 10 μM LPS. (E) Cell viability of HUVECs after incubation with different concentrations of Blank-NPs in 10 μM H_2O_2. The data are presented as mean ± SD (n=5, $^{**}P<0.01$, $^{***}P<0.001$). (F) Gene co-transfection through NPs.

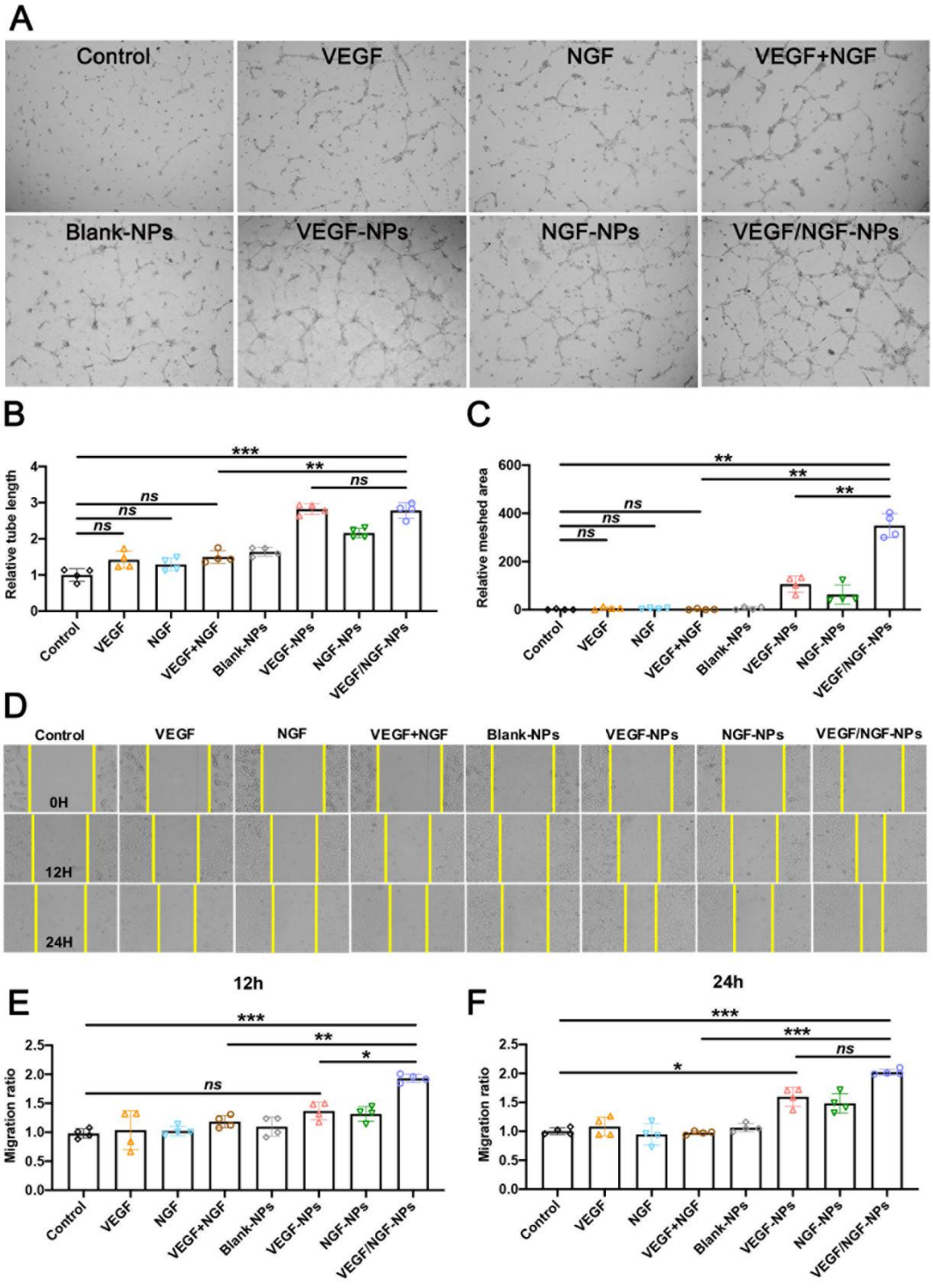

Figure 4. Effects of NPs on migration and tube fomation in HUVECs. (A) Images of tubule formation after HUVECs incubated with NPs for 6 h was observed under inverted microscop (4×). Relative tube length (B) and relative meshed area(C) were

also quantified. (D) Migration images of after HUVECs incubated with NPs for 12 h and 24 h was observed under inverted microscop (4×). Quantification of cell migration for 12 h (E) and 24 h (F) were also quantified. The data are presented as mean ± SD (n=4, $^{*}P<0.05$, $^{**}P<0.01$, $^{***}P<0.001$).

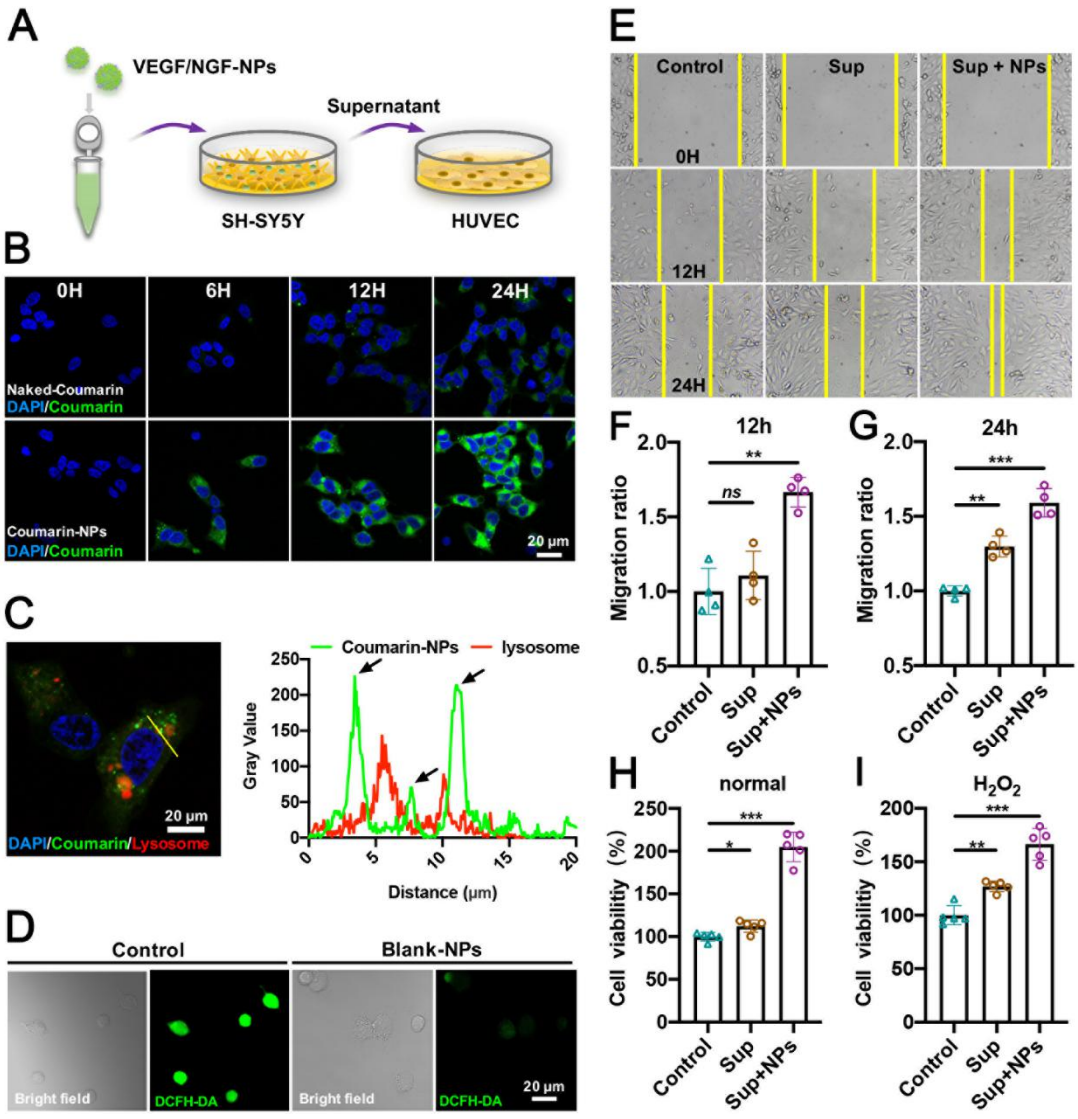

Figure 5. Enhanced interaction between SH-SY5Ys and HUVECs. (A) Schematic illustration of interaction between SH-SY5Ys and HUVECs. After SH-SY5Ys was

incubated with serum-free medium (Control), supernatant (Sup), supernatant+VEGF/NGF-NPs (Sup+NPs) for 24 h, HUVECs were incubated with supernatant for 24 h. (B) Cellular uptake of naked-Coumarin and Coumarin-NPs in SH-SY5Ys for 0 h, 6 h, 12 h, 24 h. (C) Lysosomal escape of Coumarin-NPs in SH-SY5Ys. (D) H2O2 scavenging of SH-SY5Ys after incubating Blank-NPs in 10 μM LPS. (E) Migration images of HUVECs after incubating with serum-free medium, Sup and Sup+NPs for 12 h and 24 h. Quantification of cell migration for 12 h (F) and 24 h (G) were also quantified and the data are presented as mean ± SD (n=4, **P< 0.01, ***P< 0.001). Cell viabilities of HUVECs after incubating with serum-free medium, Sup and Sup+NPs in PBS (H) and 10μM H_2O_2 (I) and the data are presented as mean ± SD (n=5, **P< 0.01, ***P< 0.001*).

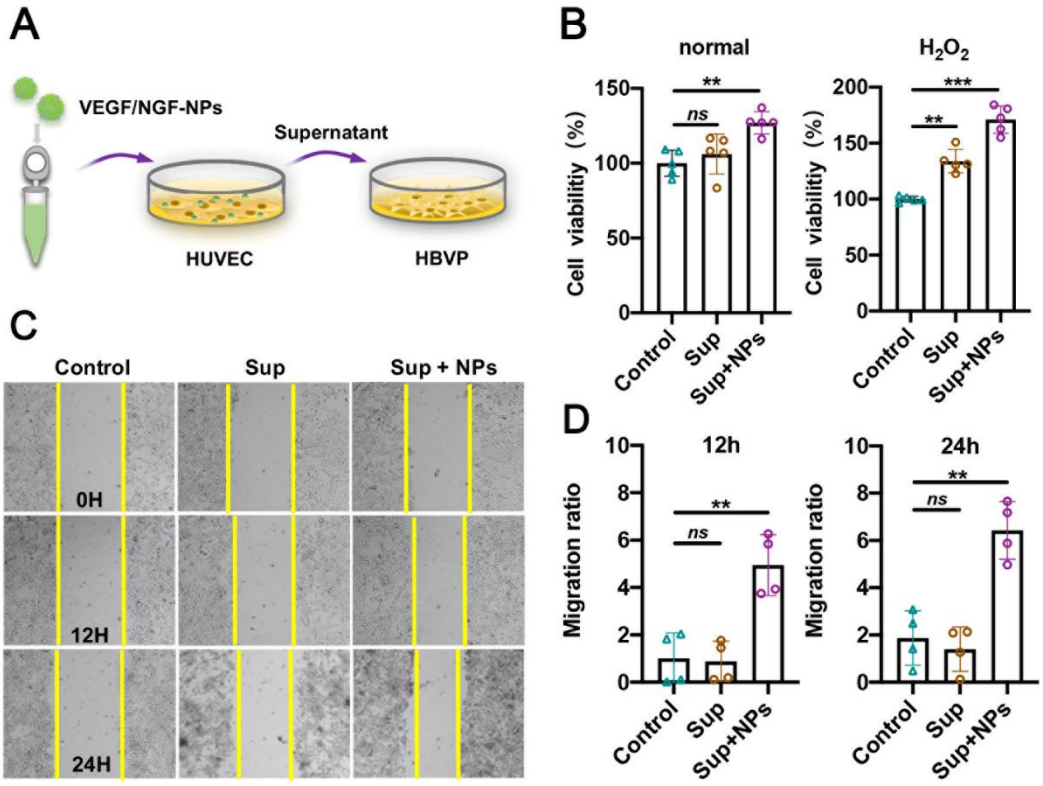

679

680 Figure 6. Enhanced interaction between HUVECs and HBVPs.

681 (A) Schematic illustration of interaction between HUVECs and HBVPs. (B) Cell

682 viabilities of HUVECs after incubating with serum-free medium, Sup and Sup+NPs

683 in PBS and H_2O_2 and the data are presented as mean ± SD (n=5, $^{**}P< 0.01$, $^{***}P<$

684 *0.001*). (C) Migration images of HBVPs after incubating with serum-free medium,

685 Sup and Sup+NPs for 12 h and 24 h. Quantification of cell migration for 12 h (F) and

686 24 h (D).

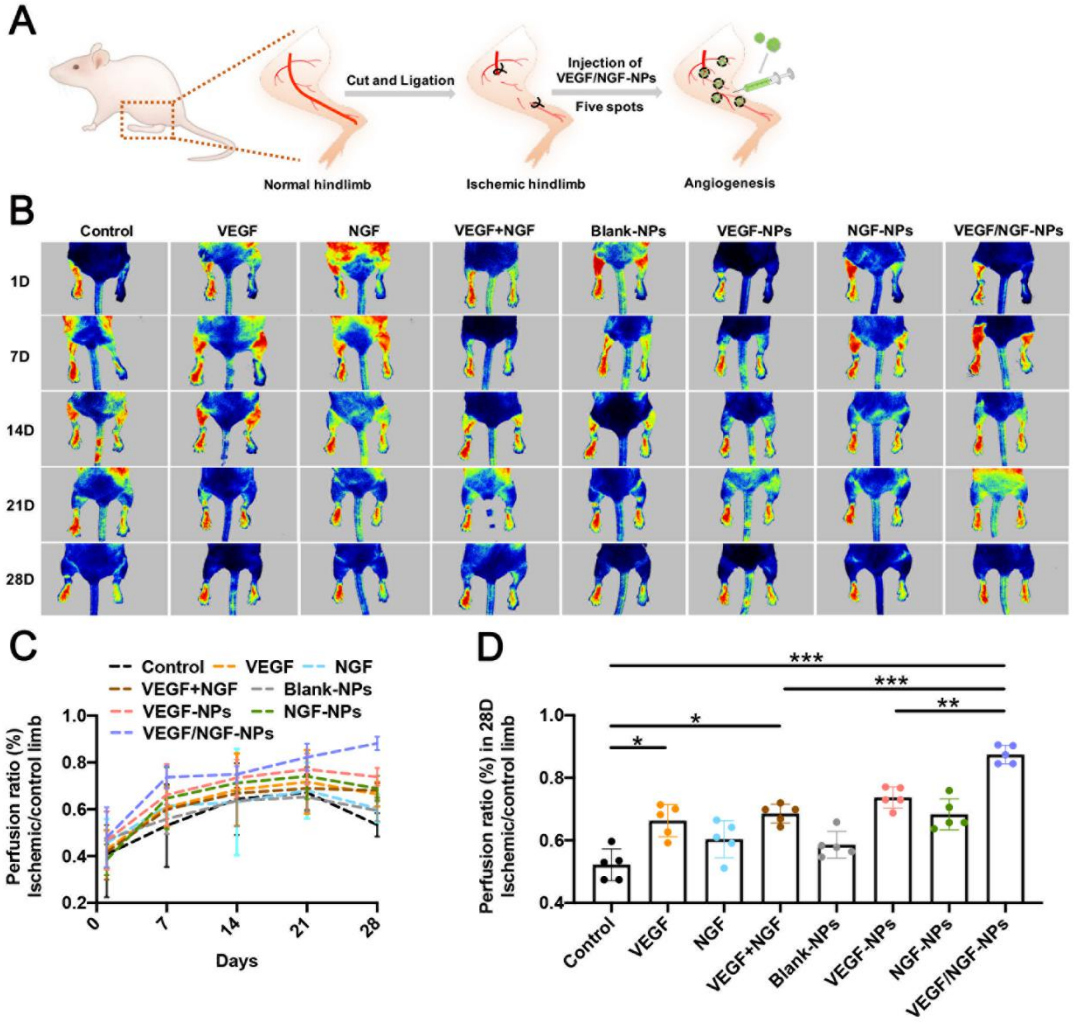

Figure 7. NPs affected blood reperfusion of the ischemic hindlimbs. (A) Schematic diagram of ischaemic hindlimb model construction and VEGF/NGF-NPs promoting angiogenesis. (B) Intramuscular injection of NPs to target blood flow recovery in ischaemic hindlimb was investigated on 28 d and representative laser doppler perfusion images were presented (n=5). And statistical difference on 28 d were also presented. The data are presented as mean ± SD (n=5, $^{*}P< 0.05$, $^{**}P< 0.01$, $^{***}P< 0.001$).

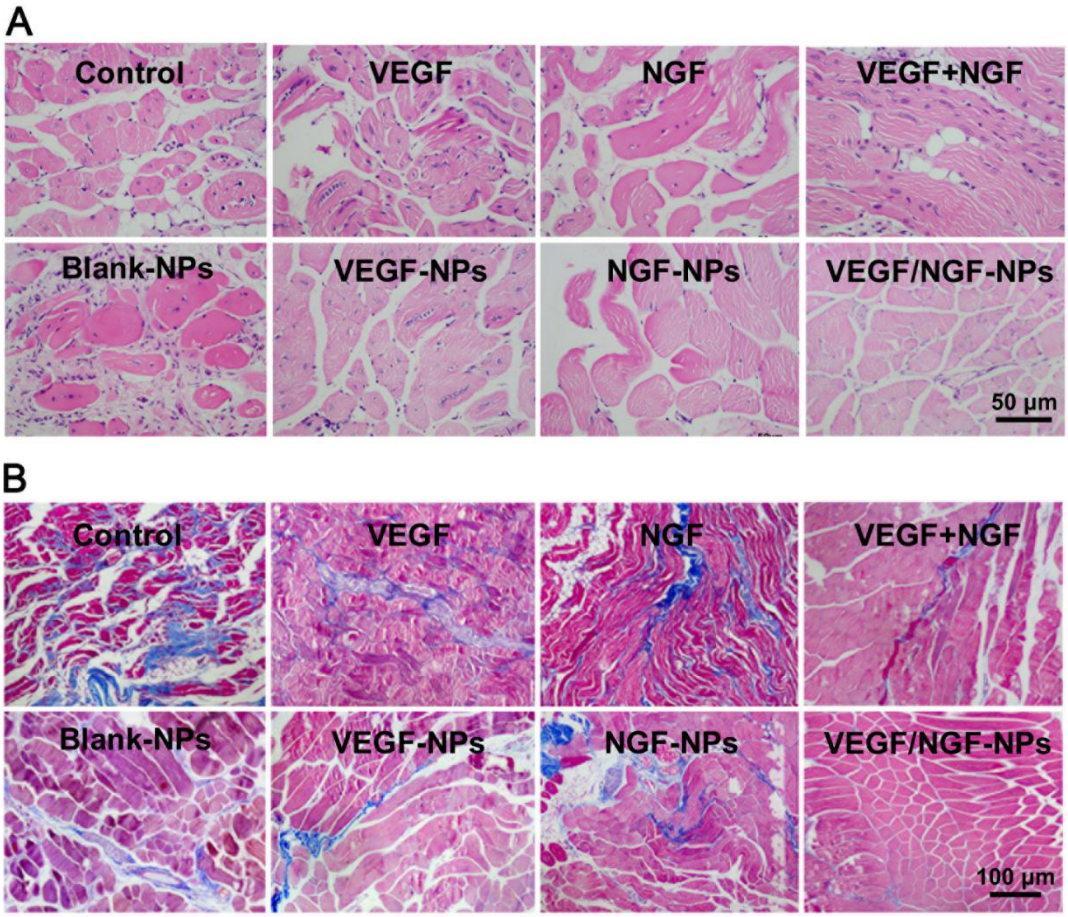

695

696 Figure 8. Histological evaluation of ischaemic hindlimb after treated by NPs.

697 Haematoxylin and Eosin (H&E) staining (A) and Masson staining (B) of ischaemic

698 hindlimb tissue treated by NPs were presented.

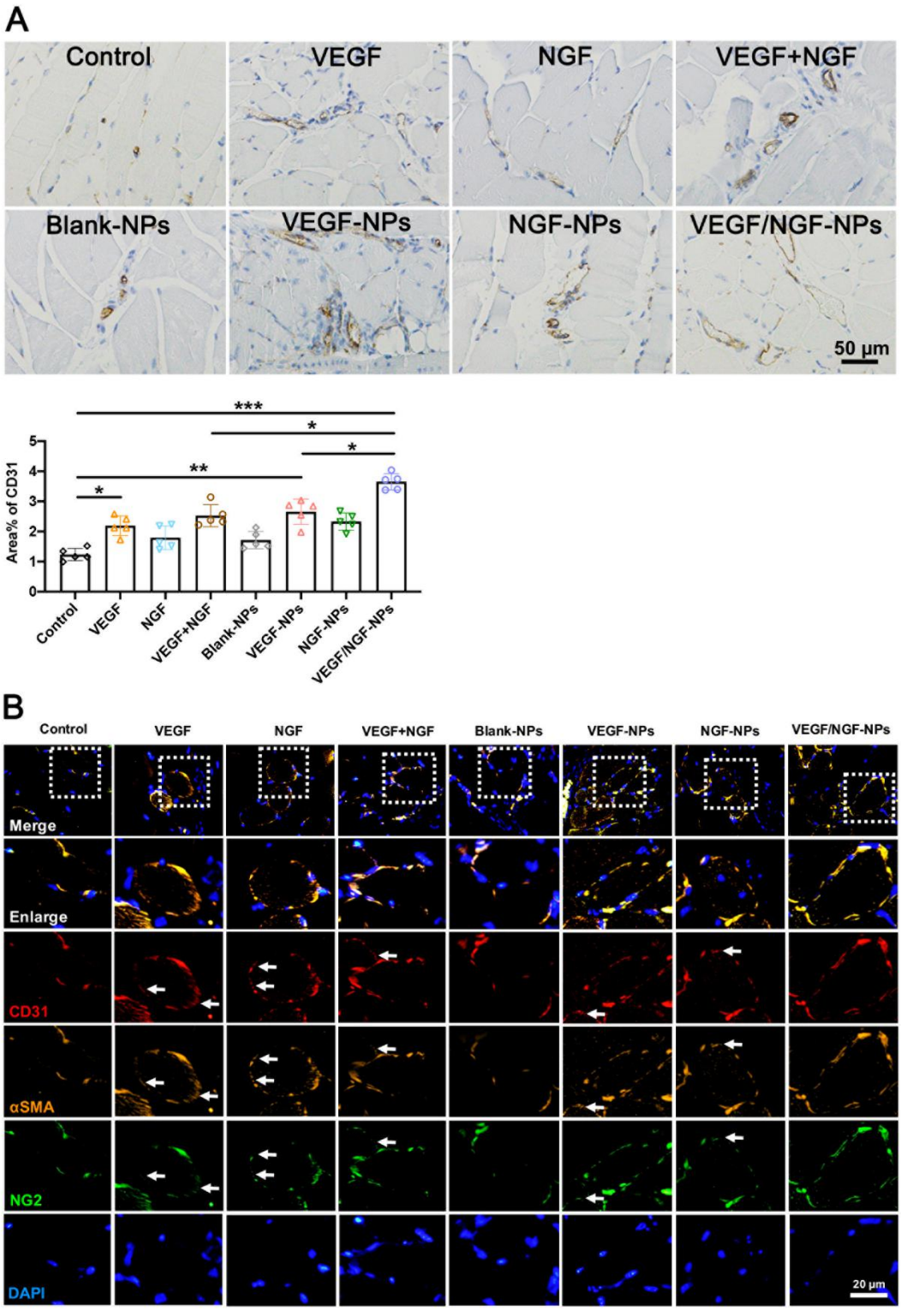

699

700 Figure 9. Angiogenesis and vascular stability of ischaemic hindlimb after treated by

701 NPs. (A) Quantification of CD31-positive areas. The data are presented as mean ± SD

(n=5, *$P<0.05$, **$P<0.01$, ***$P<0.001$). (B) Laser confocal conpositioning representative images of CD31, α-SMA, NG2 and DAPI and are prestened.

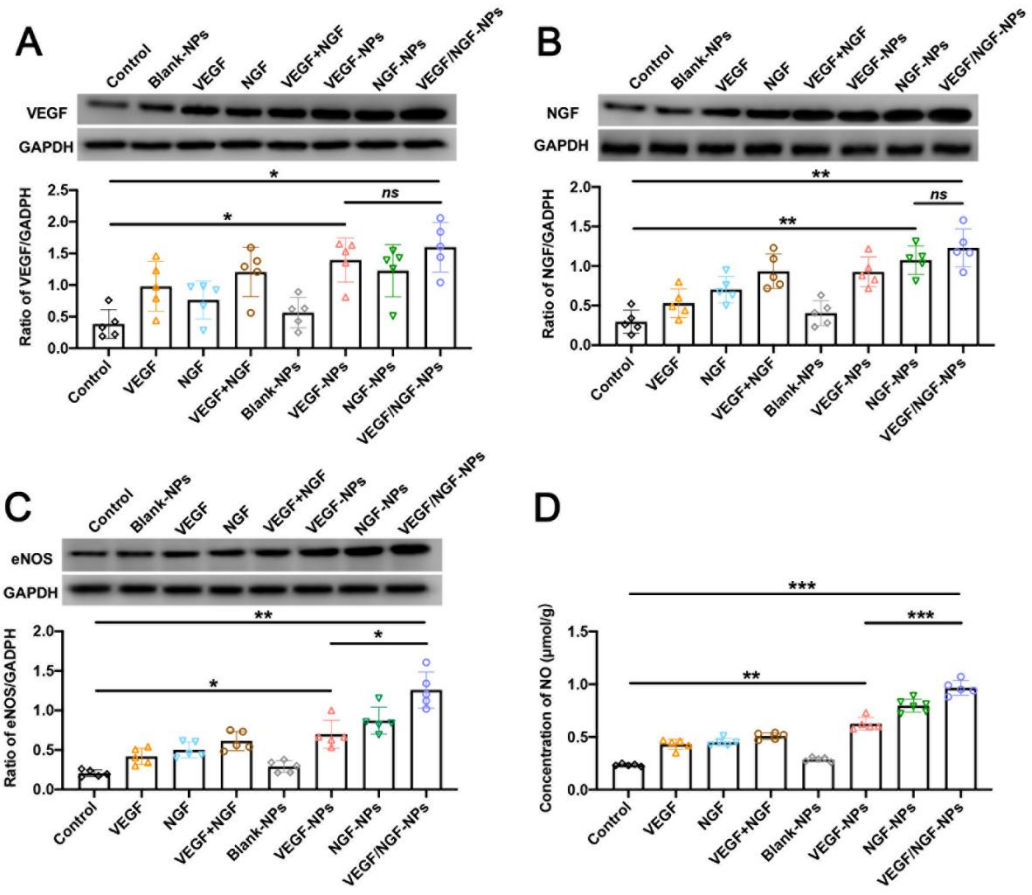

Figure 10. VEGF, NGF, eNOS and NO expression of ischaemic hindlimb after treated by NPs. Protein level alteration of VEGF (A), NGF (B), eNOS (C) was verified by western blot and NO (D) level alteration was verified by ELISA. All the data are presented as mean ± SD (n=5, *$P<0.05$, **$P<0.01$, ***$P<0.001$).

Supplementary Files

This is a list of supplementary files associated with this preprint. Click to download.

- GraphicalAbstract.docx